From GEO to LEO: First Look Into Starlink In-Flight Connectivity

Daniel Jang★, Matteo VarvelloΔ, Aravindh Raman†, Yasir Zaki★
★ New York University Abu Dhabi, Δ Nokia Bell Labs, † Cisco ThousandEyes
★ United Arab Emirates, Δ United States of America, † United Kingdom)
hsj276@nyu.edu,matteo.varvello@nokia.com,araram@cisco.com,yasir.zaki@nyu.edu

ABSTRACT

The growing demand for reliable Internet access during air travel has made in-flight connectivity (IFC) a critical service for commercial airlines. Traditional IFC systems rely on geostationary (GEO) satellites, but their high latency and limited bandwidth hinder user experience. Emerging Low Earth Orbit (LEO) constellations, such as Starlink, promise better network performance. This paper presents the first empirical comparison of IFC performance across GEO and LEO networks, using data from 26 flights operated by 7 airlines. Measurements collected via instrumented Android devices cover key metrics including latency, throughput, and CDN responsiveness. We find that Starlink's dynamic gateway selection enables shorter, more flexible routing than the static, distant gateways used by GEO systems, enhancing end-to-end performance through both shorter satellite paths and optimized ground routing. However, DNS-based content filtering on Starlink-equipped flights often affects user geolocation, introducing unnecessary terrestrial delays. We also show that the BBR congestion control algorithm delivers up to 35× higher throughput than Cubic and Vegas over Starlink, but with significantly higher retransmissions due to aggressive bandwidth probing.

1 INTRODUCTION

Commercial airlines have thus far largely relied on geostationary (GEO) satellite networks to provide connectivity to passengers. However, these networks are often affected by high latency and bandwidth constraints due to the large distances involved in signal transmission [14, 25]. In contrast, Low Earth Orbit (LEO) satellite networks, exemplified by Starlink [36], promise significant improvements in latency and overall network performance by leveraging a constellation of satellites closer to Earth.

This paper investigates the performance implications of transitioning from GEO to LEO satellite networks in the context of commercial aviation. Motivated by emerging partnerships between Starlink and major airlines [15, 30], we conducted extensive network diagnostics throughout 26 flights across 7 airlines. Our study employs `AmiGo` [40], an open-source measurement testbed on rooted Android devices to collect a comprehensive set of network performance metrics, including latency, bandwidth, DNS and CDN performance. Notably, while 20 flights operated on GEO networks, the remaining 6 were connected to Starlink's LEO network.

Our research addresses a critical gap in the literature: despite the rapid industry shift towards LEO networks, there is a scarcity of in-depth, real-world performance evaluations contrasting these architectures in the demanding environment of commercial aviation. By presenting novel empirical data, our study aims to illuminate the potential benefits and limitations of LEO networks relative to their GEO counterparts. The key findings of this paper are the following:

Static vs. Dynamic Gateway Strategies in IFC. GEO-based IFC providers rely on fixed Internet gateways, often at intercontinental distances from the airplane. In contrast, Starlink enables more flexible routes by dynamically assigning gateways (on aveage 680km away from the flight path).

Network Performance Comparison. Starlink shows substantial performance advantages over GEO-based IFC, with typical latencies under 40ms(vs GEO's 550+ms) and median downlink bandwidth of 85.2 Mbps (vs GEO's 5.9 Mbps).

DNS Configuration Impact. Starlink employs DNS-based content filtering, often using resolvers distant from the current gateway. This inflates latencies to service providers like Google and Facebook that derive client geolocation via DNS.

BBR's Performance and Tradeoffs in Starlink-Based IFC. BBR consistently outperformed Cubic and Vegas in delivery rate, achieving up to 35x higher throughput even across increasing PoP distances. However, its aggressive bandwidth probing led to significantly higher retx rates, highlighting a tradeoff between peak performance and network fairness in resource-constrained environments like IFC.

2 BACKGROUND AND RELATED WORK

Satellite Network Operators (SNOs). SNOs are broadly classified into geostationary (GEO) and Low Earth Orbit (LEO) operators. GEO satellites are positioned approximately 35,786 kilometers (km) above the equator, allowing them to maintain a fixed position relative to the Earth's surface [25]. This fixed orbital location provides consistent coverage over large areas but introduces significant latency due to the long

distance that signals must travel. In contrast, LEO SNOs operate at much lower altitudes, typically between 500-2,000 km, which greatly reduces the signal travel time and, consequently, the latency experienced by end users. Yet, this benefit comes at the cost of requiring a large constellation of satellites to ensure continuous global coverage, introducing additional complexities in network management such as frequent handovers and dynamic routing challenges [14].

SNOs for In-Flight Connectivity. Numerous SNOs provide IFC services to commercial airlines today. In the GEO domain, established providers include Inmarsat, ViaSat, SES, and Eutelsat [10, 17, 35, 41]. In the LEO arena, SpaceX's Starlink is rapidly gaining traction by offering lower latency and enhanced performance, thereby challenging the conventional GEO paradigm. Figure 1 visualizes the high-level architecture of satellite-based IFC. The end-to-end data path can be categorized into two segments: *space* and *terrestrial*. The space segment encompasses the radio signal transmission between the user terminal (mounted on aircraft) and ground station (GS). The terrestrial segment comprises the path between the ground station and the Internet backbone. Traffic here is routed through a Point of Presence (PoP), which is the gateway between the satellite and public Internet.

To the best of our knowledge, Rula et al. [33] are the first to shed some light on the performance of IFC systems at the time (2015/2016), examining both direct air-to-ground and mobile satellite service technologies. The study, based on extensive flight measurements, reveals that high latency and packet loss significantly degrade the quality of service for common internet applications. Our work revisits IFC after 8 years with focus on satellite-based services, offering timely insights into how emerging LEO networks (like Starlink) compare to traditional GEO SNOs in addressing the performance challenges previously identified.

Satellite Network Measurements. Existing research on satellite network performance has employed simulations [20, 42], active measurements [18, 19, 24, 26], collaborations with operators [29], and open platforms like M-Lab and RIPE Atlas [27, 31]. Most studies focus on single constellation types (GEO or LEO), with limited cross-constellation comparisons typically using public datasets and stationary user terminals.

3 METHODOLOGY

Measurement Overview. We build on the `AmiGo` framework [40], an open source testbed design which relies on travelers carrying mobile phones to act as vantage points. `AmiGo` includes a control server for remote management of mobile measurement endpoints (MEs). The server exposes RESTful APIs that the MEs use to report their status (e.g., battery level and network connectivity) and fetch instrumentation code. These MEs are rooted Android devices configured

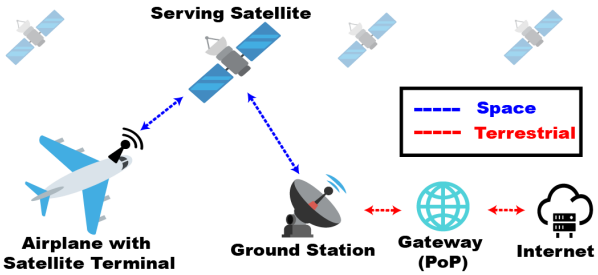

Figure 1: End-to-end IFC client to Internet path.

using `termux` [38]. MEs collect various network metrics, including download/upload throughput and latency measured via Speedtest [28] (*i.e.,* relying on Ookla servers), and latency and network paths towards major content providers such as Cloudflare and Google. ME also run experiments to evaluate popular DNS and CDN providers.

Starlink Extension. We extend `AmiGo` to analyze the performance differences between Starlink's various Points of Presence (PoPs) and their impact on network latency. In consumer Starlink terminals, the gRPC interface typically provides network diagnostics including real-time latency measurements to the gateway [37, 43]. However, gRPC queries were not permitted during our measurement flights.

We instead deploy cloud servers in multiple AWS regions strategically located along the flight path. This allows MEs to conduct high-frequency (10 ms granularity) UDP ping measurements via IRTT [16] to the *closest* AWS server, *i.e.,* co-located to the current PoP used. Each measurement session runs for 5 minutes, providing time-series data for fine-grained comparison of latency characteristics across PoPs.

We further piggyback on these AWS servers to evaluate TCP performance. Specifically, we performed file transfers under different TCP congestion control algorithms (CCAs), configured using `sysctl` [21] at the AWS server. We rely on a simple *receiver* which runs in the ME and is instrumented to open a connection towards a server. The *sender* runs in AWS and accepts connections and transfer test files of a desired size. During each file transfer, fine-grained socket statistics are collected at the server via `ss` [22]. ME automatically runs the two tests sequentially when it connects to a new PoP.

Finally, we retrieve fine-grained aircraft position data from an online flight-tracking service [11]. Since each commercial flight has a unique ID that generally follows a consistent route, we estimate its path using previous route data. These projected paths allow us to identify anticipated Starlink PoPs and corresponding AWS regions for the two aforementioned measurements. We also use the position data to correlate network performance with aircraft location.

Data Collection. We run the measurements from December 2023 to April 2025, recruiting 10 volunteers who traveled on

SNO	ASN	Airline	PoPs(s)
Inmarsat	AS31515	Qatar Airways	Staines (UK) Greenwich (US)
Intelsat	AS22351	KLM Airlines Air France	Wardensville (US)
Panasonic	AS64294	Etihad Airways Air France	Lake Forest (US)
SITA	AS206433	Etihad Airways Qatar Airways	Amsterdam (NL)
		Emirates Saudia	Lelystad (NL)
ViaSat	AS40306	JetBlue Airways	Englewood (US)
Starlink	AS14593	Qatar Airways	*Table 3 in Appendix*

Table 1: Satellite Network Operators measured.

commercial airplanes equipped with in-flight WiFi. Each volunteer carried an `AmiGo` ME (Samsung Galaxy A34 5G [13]) to run network measurements during the flight. Volunteers were instructed to carry these devices and refrain from using them to avoid interference with the measurements.

Our dataset comprises 20 flights with GEO SNOs recorded between December 2023 and March 2025, spanning 7 airlines operating across 22 airports in 15 countries. Details of these flights are summarized in the Appendix (see Table 5). In addition, we began our investigation of Starlink Aviation in March 2025, following its initial deployment on Qatar Airways in November 2024 [30]. This portion of our dataset includes 6 Qatar Airways flights: 2 DOH-JFK, 2 JFK-DOH, 1 DOH-LHR, and 1 LHR-DOH route. Note that Starlink Aviation remains in the early adoption phase, available only on limited flight paths and airplane models. For Qatar Airways, the service is scheduled to be available on just 40 Boeing 777s (17% of their fleet) serving 28 airports by June 2025 (15% of their 181 international destinations) [6, 7, 9].

We utilized the Starlink extension of `AmiGo` only for the final two flights between Doha and London, after discovering that the operator's gRPC interface was inaccessible during the earlier flights. We instrumented AWS EC2 t3.xlarge instances [8] close to intercepted PoPs: London (eu-west-2), Milan (eu-south-1), Frankfurt (eu-central-1), and UAE (me-central-1)—, reflecting connections to Starlink PoPs in London, Milan, Frankfurt, Sofia, Warsaw, and Doha observed in our dataset. There is currently no AWS region in reasonable proximity to Sofia and Warsaw.

4 STARLINK VS GEO

4.1 Tomography of Public Gateways

For GEO clients, we find that only one or two PoPs are used per flight, thus often geographically distant from the aircraft's position. Table 1 summarizes the PoP locations observed across all GEO-based flights in our dataset. Figure 2 maps this behavior during a Qatar Airways flight from Doha

Figure 2: Flight path and PoP locations during Doha-Madrid route, November 2024. The aircraft utilized Inmarsat (AS31515).

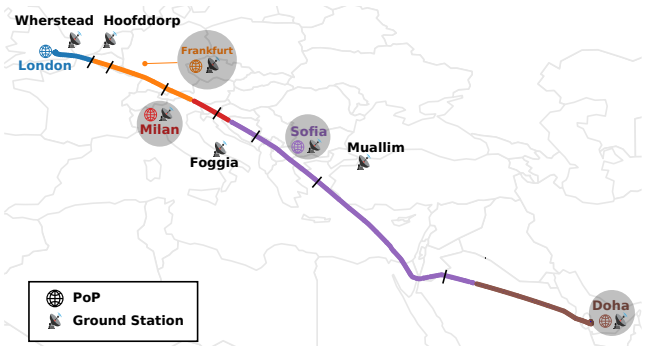

Figure 3: Doha–London flight path (Apr 2025) color-coded by Starlink PoP. Segments closest to each ground station (GS) are marked by black vertical lines. Grey circles indicate cities where PoP and GS are co-located.

to Madrid in November 2024, where the client connected via Inmarsat (AS31515, GEO). Throughout the 7-hour journey, all traffic was routed through two PoPs located in Staines (UK), and Greenwich (US), approximately 7,380 km away from the flight path at its furthest point.

In contrast, Starlink employs a dynamic approach to PoP assignment based on aircraft position. Figure 3 shows an example with a Qatar Airways flight from Doha to London in April 2025, where the client's traffic was routed through five Starlink PoPs. The flight's trajectory is color-coded to indicate which PoP was used during each segment of the journey. The map shows that PoPs were utilized for significantly varying time periods. The Sofia PoP maintained the longest connection, serving approximately 3 hours and covering over 2,700 kilometers of the flight path, while the Milan PoP provided connectivity for only about 22 minutes, covering just 330 kilometers. PoP transitions did not always follow simple geographic proximity rules. For instance, the connection switched from Doha to Sofia despite Doha remaining closer to the aircraft at the transition point. We observed these patterns across all 6 Starlink flights in our dataset, with their details of PoP usage provided in the Appendix (Table 3).

To provide a potential explanation of the previous behavior, Figure 3 also maps the locations of Starlink's ground stations (GS) obtained from crowd-sourced datasets [12, 34]. By identifying the geographically closest GS along the flight path, we conjecture that PoP selection could be primarily determined by GS availability rather than direct aircraft-to-PoP

PoP	Google	FB	jsDelivr (Fastly)	jsDelivr (Cloudf.)	jQuery	Cloudf.
Doha	LDN AMS	LDN MRS	LDN	DOH	MRS	DOH SIN
Sofia	LDN AMS FRA	LDN PAR MRS	LDN	SOF	SOF	SOF
Milan	LDN AMS FRA	LDN PAR	LDN		MXP SOF MAD FRA	MXP SOF MAD
Frankfurt	LDN AMS	LDN PAR	LDN	FRA	FRA	FRA
Madrid	LDN FRA	LDN	LDN	MAD	MAD	MAD
London	LDN AMS	LDN	LDN	LDN	LDN	LDN
NY	NYC	NYC	NYC	NYC	NYC	NYC

Table 2: Cache location per provider and Starlink PoP, inferred from airport codes in traceroute (Google, Facebook) and HTTP headers (jQuery, jsDelivr, Cloudflare).

proximity. As a hypothetical example, when the plane was within range of the Doha GS, it was assigned to the Doha PoP. Later, as the flight progressed, the clients switched to Sofia PoP when the Muallim (Turkey) GS became the nearest.

4.2 DNS Configuration

In-flight connectivity providers commonly employ DNS filtering to restrict access to bandwidth-intensive or blacklisted domains. We used NextDNS [2] to identify the DNS resolvers used throughout the flights. NextDNS operates as an authoritative DNS service for custom domains with a time-to-live (TTL) of zero, ensuring that resolvers always query it – granted that TTL is respected. It then echoes back to its users the unicast address of the resolver that made the request. This allows us to geolocate the resolver's IP address even when anycast is used between client and resolver.

We detail DNS resolvers and locations for GEO SNOs in the Appendix (see Table 4). We identified 7 unique DNS hosts across the GEO SNOs, with ViaSat and SITA employing their own DNS servers. Most DNS resolvers were located within the same country as the client's PoP, except for Inmarsat which temporarily used Packet Clearing House (Amsterdam) despite its current PoP being in Staines (England).

Conversely, all the Starlink-based flights in our dataset used CleanBrowsing [4], a popular DNS filtering technology for safe browsing. CleanBrowsing uses anycast to direct users to the nearest DNS resolver, ideally located near the PoP used by Starlink at a given time (see Figure 3, for example). However, with only 50 anycast locations globally [1], CleanBrowsing often introduces considerable path inflation between PoP and DNS resolver. For example, during flights over Europe, DNS queries are mostly resolved via London, even when using the Sofia PoP, located 1,700 km away.

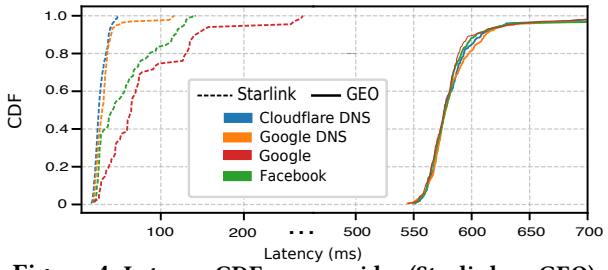

Figure 4: Latency CDF per provider (Starlink vs GEO).

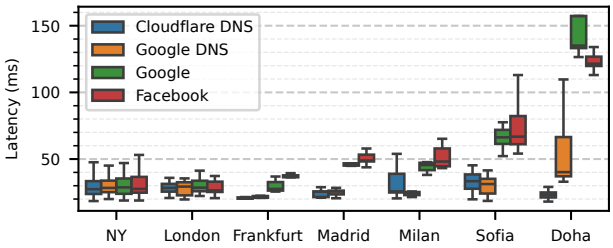

Figure 5: Latency to service providers per Starlink PoP.

4.3 Network Performance

Latency. Using traceroute data, Figure 4 compares latency of GEO-based IFC and Starlink to four global service providers: two DNS services (Cloudflare, Google DNS) and two content providers (Google, Facebook). GEO SNOs consistently show latencies about an order of magnitude longer, with over 99% of 1,228 tests exceeding 550 ms. In contrast, Starlink shows much lower delays: 90% of 320 DNS traceroutes resolve within 40 ms, while 83.5% of 97 tests to Facebook and 74.6% of 67 to Google are under 100 ms.

For Starlink, Figure 4 shows high latencies to Google and Facebook compared to Cloudflare and Google DNS. Given all these providers have global infrastructures, we would normally expect similar latency performance. However, a key distinction lies in how traceroute is executed. For Google and Cloudflare DNS, traceroute targets (anycast) IP addresses (8.8.8.8 and 1.1.1.1), thus bypassing DNS resolution. In contrast, traceroutes to Google and Facebook begin with a DNS lookup, which returns an IP address based on the geolocation of the DNS resolver in use. Starlink usage of CleanBrowsing introduces a geolocation mismatch, e.g., redirecting traffic to London despite being connected to Doha (see Table 2), causing inefficiencies in the terrestrial path.

We show that such DNS configuration introduced additional delay in Figure 5, which breaks down the Starlink latency results from Figure 4 by PoP. For New York and London PoPs, latency across all providers is consistently low, averaging approximately 29 ms. For the remaining PoPs, latencies to Google and Facebook were inflated due to CleanBrowsing DNS geolocation inefficiencies. This latency inflation

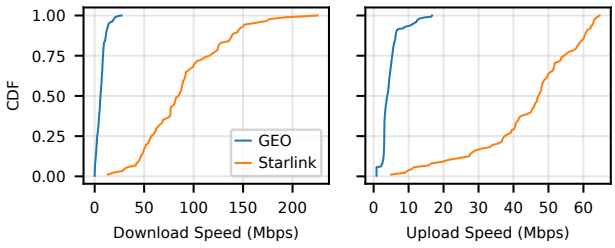

Figure 6: Downlink (left) and uplink (right) bandwidth: Starlink vs. GEO (Ookla speedtests).

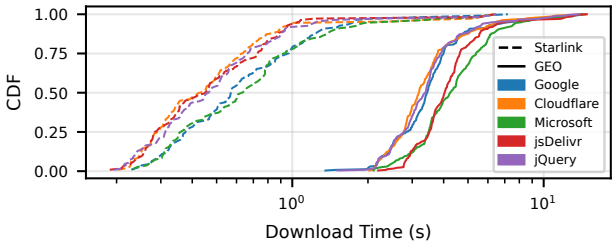

Figure 7: CDF of download time for jQuery library across CDNs, with results from Starlink and GEO SNOs shown in dashed lines and solid lines, respectively.

largely increases with distance from the resolver's geolocation, resulting in 1.2× (Frankfurt) to 4.6× (Doha) higher delays compared to those observed in NY and London PoPs.

Bandwidth. We use Ookla speedtests [28] to measure IFC bandwidth. Figure 6 compares download and upload CDFs between Starlink and GEO SNOs. Similar to latency results, Starlink consistently achieves higher bandwidth. For download, Starlink showed a median of 85.2 Mbps with an IQR of 60.2 Mbps, significantly outperforming GEO SNOs, which had a median of only 5.9 Mbps with an IQR of 5.7 Mbps. Notably, 83% of tests with GEO SNOs recorded download speeds below 10 Mbps, less than Starlink's minimum observed downlink at 18.6 Mbps. The performance gap is similarly substantial for uplink, where Starlink achieved a median of 46.6 Mbps with an IQR of 17.8 Mbps, while GEO providers delivered a median of just 3.9 Mbps with an IQR of 2.2 Mbps.

To explore how the choice of SNO impacts application-layer performance and content delivery for IFC, we measure the download time for `jquery.min.js` (a popular JavaScript library [39]) from five global CDN providers. Figure 7 presents the CDF of download times, comparing results from 1,423 tests with GEO SNOs (solid lines) and 547 tests with Starlink (dashed lines). For GEO SNOs, the fastest download time was recorded at 1.35 seconds, with 96.7% of tests requiring 2-10 seconds. In contrast, Starlink demonstrated dramatically better performance across all CDN providers, with over 87% of download tests completing in under one second. The intersection of the two CDF tails in the figure shows that ~7% of the slowest Starlink downloads lasted longer than

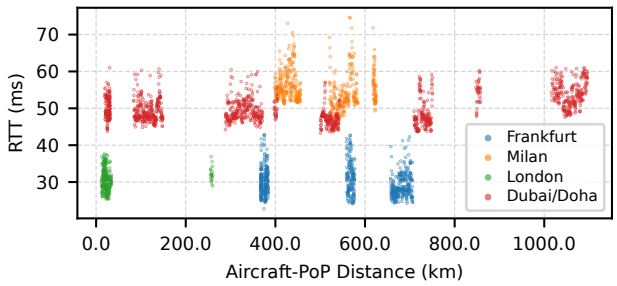

Figure 8: Latency (to closest AWS server) as a function of airplane's distance to Starlink PoP in use.

the fastest GEO downloads for each CDN. These Starlink outliers suffered from long DNS resolution times, which accounted for 74% of the total download duration, on average; this is likely a result of DNS cache misses requiring recursive resolution via authoritative nameservers.

Finally, we analyze the impact of DNS-based geolocation errors on CDN providers accessed from Starlink IFC. Table 2 summarizes cache node locations inferred from geographic identifiers in HTTP headers (e.g., `x-served-by` from Fastly, `cf-ray` from Cloudflare) [3, 5]. We examined jQuery (Fastly), jsDelivr (Fastly and Cloudflare), and direct Cloudflare tests. Requests via Cloudflare, both direct and through jsDelivr, were routed to caches near the Starlink PoP, thanks to BGP anycast-based routing that bypasses DNS-based geolocation errors. Similar cache selection is achieved by jQuery, using Fastly's anycast. In contrast, jsDelivr requests served by Fastly were routed to London, regardless of PoP, suggesting DNS-based cache selection. This routing mismatch impacted performance: jsDelivr over Cloudflare was 34.7% faster on average than over Fastly (Mann-Whitney U, $p < 0.05$).

5 A CLOSER LOOK AT STARLINK

In this section, we focus on Starlink Aviation using data from 2 Qatar Airways flights on the Doha-London route, where we employed AWS endpoints to conduct high-frequency UDP `ping` as well as TCP file transfers. We first examine the latency impact of Starlink dynamic gateway selection, followed by implications of TCP CCA.

5.1 Location-Based Delay

We define *plane-to-PoP* distance as the haversine distance between the plane's ground projection and the current PoP in use. Figure 8 shows RTT to the closest AWS server to each PoP (filtered below 95th percentile to exclude outliers) as a function of plane-to-PoP distance. Each colored cluster represents a set of high frequency pings (IRTT) conducted while connected to the PoP indicated by the color, e.g., red for Doha approximated by the closest AWS server (Dubai).

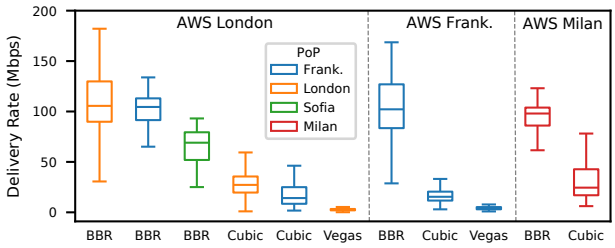

Figure 9: Delivery rate from AWS servers to clients using different Starlink PoPs and TCP CCAs.

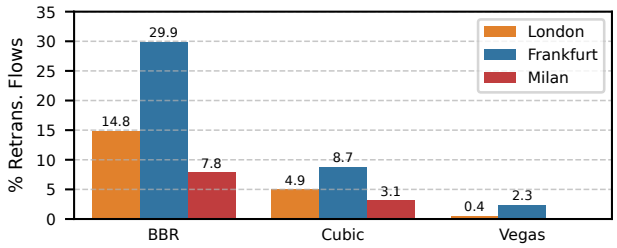

Figure 10: % of retransmissions flows by location and CCA

The Doha PoP (red) has the most number of tests since it was utilized longer than other PoPs (see Figure 3). Note that while the Sofia PoP was used even longer, no AWS server is available in the region, so no IRTT measurement was run for this PoP. The figure shows that Milan (orange) and Doha (red) PoPs exhibit significantly higher latency (with medians of 54.3 ms and 49.1 ms, respectively) compared to London (green) and Frankfurt (blue) PoPs (with medians of 30.5 ms and 29.5 ms, respectively). This latency difference persisted regardless of the physical distance between aircraft and PoP. Latency measurements to Starlink PoPs (traceroute hops with address 100.64.0.1) reveal statistical correlation with distance only beyond 800 km ($r = 0.698$, $p < 0.0001$).

To further explain the previous result, we examine differences in peering arrangements. Milan and Doha PoPs route traffic through intermediaries (AS57463 and AS8781) which induces additional latency. In contrast, London and Frankfurt PoPs establish direct peering relationships with major service providers, eliminating these intermediary hops. We cross-validated these findings using data from Ripe Atlas [32], analyzing traceroutes to Facebook and Google conducted from probes using the same Frankfurt, London, and Milan Starlink PoPs (no probe using the Doha PoP was available) from March 1st to April 20th, 2025. Out of 9,598 traceroutes originating from the Milan POP, 95.4% included traversals to transit providers. This stood in stark contrast to Frankfurt and London POPs, which exhibited such patterns in only 0.09% of 9,583 and 1.7% of 9,596 traceroutes, respectively.

5.2 TCP Performance

We here analyze TCP performance from file transfer tests, where different AWS servers were selected as endpoints based on the Starlink PoP in use. We evaluate three popular CCAs: BBR, Cubic, and Vegas. We prioritized using the closest available server to each PoP, but also included London for Frankfurt and Sofia to assess distance effects on CCA performance. Certain PoPs could not test all CCAs due to constraints: Sofia lacks a nearby AWS region, and Milan's short connection window prevented Vegas tests (Appendix Table 6 summarizes the experimental setups).

Figure 9 plots the delivery rates obtained across all tests, organized by AWS server location and color-coded by PoP. For tests when server and PoP were geographically aligned (ex: London-London), BBR consistently outperforms other CCAs, achieving median delivery rates of 98-105 Mbps, roughly 3-6x higher than Cubic and 24-35x higher than Vegas. The figure also shows that BBR's performance gradually degrades as PoP distance increases. Comparing results in London AWS accessed through London, Frankfurt, and Sofia PoPs, the median (IQR) delivery rate drops from 105.5 (40) Mbps to 104.5 (21) Mbps to 69 (27) Mbps, respectively. However, BBR remains superior to what Cubic (15.4-27.2 Mbps) and Vegas (<5 Mbps) achieves even in geographically aligned conditions.

The goodput discrepancies can be attributed to BBR's aggressive window management strategy, which directly estimates bandwidth and RTT to model network capacity, making it resilient to random packet losses and variable latencies that challenge loss-based (Cubic) and delay-based (Vegas) CCAs in satellite networks. However, our results also highlight potential tradeoffs prompted by BBR's high bandwidth utilization. We analyze retransmission by computing *retransmission flow %*, or the proportion of 100 ms intervals containing retransmitted packets in pcap captures. Figure 10 compares the retransmission flow of CCAs for tests conducted in geographically aligned server-PoP pairs. BBR exhibits significantly higher retransmission rates than its counterparts; 3-34.3× higher in London, 3.4-12.8× in Frankfurt (peaking at 29.8%), and 2.5× in Milan. These elevated retransmissions suggest that BBR tends to overestimate available capacity in Starlink networks, causing buffer overflow and subsequent packet loss [23]. These characteristics raise network fairness concerns in resource-constrained environments like IFC, where BBR flows might monopolize limited satellite bandwidth.

6 CONCLUSION

We present the first in-situ characterization of Starlink Aviation, comparing its performance with GEO-based in-flight connectivity (IFC) across 26 flights operated by 7 commercial airlines. Unlike GEO providers that rely on fixed PoPs, Starlink's dynamic PoP assignment consistently shortens the

satellite bent-pipe throughout flight paths. Consequently, we find that variations in end-to-end latency largely stem from terrestrial factors, particularly peering relationships and geolocation inefficiencies due to DNS-based content filtering, rather than from plane-PoP proximity. Finally, we show that BBR achieves higher delivery rates than Cubic and Vegas, but with increased retransmissions. These results highlight both the promise and current limitations of LEO satellite networks for IFC.

REFERENCES

[1] [n. d.]. CleanBrowsing Network Status. https://cleanbrowsing.org/status/

[2] [n. d.]. NextDNS. https://nextdns.io/

[3] [n. d.]. X-Served-By | Fastly Documentation. https://www.fastly.com/documentation/reference/http/http-headers/X-Served-By/

[4] 2025. *CleanBrowsing | DNS Filtering Platform.* https://cleanbrowsing.org/ Accessed: 2025-05-04.

[5] 2025. Cloudflare HTTP headers. https://developers.cloudflare.com/fundamentals/reference/http-headers/

[6] Qatar Airways. [n. d.]. Fleet Qatar Airways. https://www.qatarairways.com/en/fleet.html

[7] Qatar Airways. [n. d.]. Starlink. The fastest on-board Wi-Fi in the sky | Qatar Airways. https://www.qatarairways.com/en-ae/onboard/connectivity.html

[8] Amazon Web Services. 2025. *Amazon EC2 T3 Instances.* Amazon Web Services. https://aws.amazon.com/ec2/instance-types/t3/ Accessed: 2025-05-06.

[9] Flight Connections. 2025. Qatar Airways Flights and Destinations - FlightConnections. https://www.flightconnections.com/route-map-qatar-airways-qr

[10] Eutelsat. 2021. *Aviation Inflight Connectivity.* https://www.eutelsat.com/en/satellite-communication-services/aviation-inflight-connectivity.html

[11] Flightradar24 AB. 2025. *Flightradar24.* https://www.flightradar24.com/ Accessed April 28, 2025.

[12] Google My Maps user. 2025. Unofficial Starlink Global Gateways & PoPs. https://www.google.com/maps/d/u/0/viewer?mid=1805q6rlePY4WZd8QMOaNe2BqAgFkYBY&hl=en_US&ll=29.92773521630133%2C35.02090615416515&z=4 Accessed April 29, 2025.

[13] GSMArena. 2023. *Samsung Galaxy A34 - Full phone specifications.* GSMArena.com. https://www.gsmarena.com/samsung_galaxy_a34-12074.php

[14] Mark Handley. 2018. Delay is Not an Option: Low Latency Routing in Space. In *Proceedings of the 17th ACM Workshop on Hot Topics in Networks* (Redmond, WA, USA) *(HotNets '18)*. Association for Computing Machinery, New York, NY, USA, 85–91. https://doi.org/10.1145/3286062.3286075

[15] Hawaiian Airlines. 2025. Hawaiian Airlines Now Offering Fast and Free Starlink Wi-Fi Across Entire Airbus Fleet. https://newsroom.hawaiianairlines.com/releases/hawaiian-airlines-now-offering-fast-and-free-starlink-wi-fi-across-entire-airbus-fleet Accessed: 2025-03-13.

[16] Paul Heist. 2025. Isochronous Round-Trip Tester (IRTT). https://github.com/heistp/irtt. Accessed: 2025-04-22.

[17] Inmarsat. 2023. *Inmarsat plans fastest inflight broadband for business aviation.* https://www.inmarsat.com/en/news/latest-news/aviation/2023/fastest-inflight-broadband-plans-for-business-aviation.html

[18] Liz Izhikevich, Manda Tran, Katherine Izhikevich, Gautam Akiwate, and Zakir Durumeric. 2024. Democratizing LEO Satellite Network Measurement. *Proc. ACM Meas. Anal. Comput. Syst.* 8, 1, Article 13 (Feb. 2024), 26 pages. https://doi.org/10.1145/3639039

[19] Mohamed M. Kassem, Aravindh Raman, Diego Perino, and Nishanth Sastry. 2022. A Browser-side View of Starlink Connectivity. In *Proceedings of the 22nd ACM Internet Measurement Conference (IMC'22)*. Nice, France.

[20] Simon Kassing, Debopam Bhattacherjee, André Baptista Águas, Jens Eirik Saethre, and Ankit Singla. 2020. Exploring the "Internet from space" with Hypatia. In *Proceedings of the ACM Internet Measurement Conference* (Virtual Event, USA) *(IMC '20)*. Association for Computing Machinery, New York, NY, USA, 214–229. https://doi.org/10.1145/3419394.3423635

[21] Michael Kerrisk. [n. d.]. *sysctl(8) - Linux manual page.* Linux man-pages project. https://man7.org/linux/man-pages/man8/sysctl.8.html Accessed: April 30, 2025.

[22] Michael Kerrisk et al. 2025. *ss(8) - Linux manual page.* https://man7.org/linux/man-pages/man8/ss.8.html Accessed April 28, 2025.

[23] Zeqi Lai, Zonglun Li, Qian Wu, Hewu Li, Weisen Liu, Yijie Liu, Xin Xie, Yuanjie Li, and Jun Liu. 2024. Mind the Misleading Effects of LEO Mobility on End-to-End Congestion Control. In *Proceedings of the 23rd ACM Workshop on Hot Topics in Networks* (Irvine, CA, USA) *(HotNets '24)*. Association for Computing Machinery, New York, NY, USA, 34–42. https://doi.org/10.1145/3696348.3696867

[24] Sami Ma, Yi Ching Chou, Haoyuan Zhao, Long Chen, Xiaoqiang Ma, and Jiangchuan Liu. 2023. Network Characteristics of LEO Satellite Constellations: A Starlink-Based Measurement from End Users. In *IEEE INFOCOM 2023 - IEEE Conference on Computer Communications*. 1–10. https://doi.org/10.1109/INFOCOM53939.2023.10228912

[25] Gérard Maral, Michel Bousquet, and Zhili Sun. 2020. *Satellite Communications Systems: Systems, Techniques and Technology* (6th ed.). Wiley.

[26] François Michel, Martino Trevisan, Danilo Giordano, and Olivier Bonaventure. 2022. A first look at starlink performance. In *Proceedings of the 22nd ACM Internet Measurement Conference*. 130–136.

[27] Nitinder Mohan, Andrew E. Ferguson, Hendrik Cech, Rohan Bose, Prakita Rayyan Renatin, Mahesh K. Marina, and Jörg Ott. 2024. A Multifaceted Look at Starlink Performance. In *Proceedings of the ACM Web Conference 2024* (Singapore, Singapore) *(WWW '24)*. Association for Computing Machinery, New York, NY, USA, 2723–2734. https://doi.org/10.1145/3589334.3645328

[28] OOKLA. 2024. Speedtest CLI, Internet connection measurement for developers. https://www.speedtest.net/apps/cli.

[29] Daniel Perdices, Gianluca Perna, Martino Trevisan, Danilo Giordano, and Marco Mellia. 2022. When satellite is all you have: watching the internet from 550 ms. In *Proceedings of the 22nd ACM Internet Measurement Conference* (Nice, France) *(IMC '22)*. Association for Computing Machinery, New York, NY, USA, 137–150. https://doi.org/10.1145/3517745.3561432

[30] Qatar Airways. 2025. Qatar Airways Equips 30th Boeing 777 with Starlink, Outpacing Original Timeline by 70 Per Cent. https://www.qatarairways.com/press-releases/en-WW/247298-qatar-airways-equips-30th-boeing-777-with-starlink-outpacing-original-timeline-by-70-per-cent Accessed: 2025-03-13.

[31] Aravindh Raman, Matteo Varvello, Hyunseok Chang, Nishanth Sastry, and Yasir Zaki. 2023. Dissecting the Performance of Satellite Network Operators. In *Proceedings of the 19th International Conference on emerging Networking EXperiments and Technologies (CoNEXT'23)*. Paris, France.

[32] RIPE NCC. [n. d.]. RIPE Atlas. https://atlas.ripe.net/. Accessed: 2025-04-27.

[33] John P. Rula, James Newman, Fabián E. Bustamante, Arash Molavi Kakhki, and David Choffnes. 2018. Mile High WiFi: A First Look

At In-Flight Internet Connectivity. In *Proceedings of the 2018 World Wide Web Conference* (Lyon, France) *(WWW '18)*. International World Wide Web Conferences Steering Committee, Republic and Canton of Geneva, CHE, 1449–1458. https://doi.org/10.1145/3178876.3186057

[34] satellitemap.space. 2025. *Live Starlink Satellite and Coverage Map.* https://satellitemap.space/ Accessed April 29, 2025.

[35] SES. 2024. *SES Launches SES Open Orbits™ Inflight Connectivity Network.* https://www.ses.com/press-release/ses-launches-ses-open-orbitstm-inflight-connectivity-network

[36] Starlink. 2025. Starlink Aviation - High-Speed, Low-Latency Inflight Internet. https://www.starlink.com/business/aviation Accessed: 2025-03-13.

[37] Hammas Bin Tanveer, Mike Puchol, Rachee Singh, Antonio Bianchi, and Rishab Nithyanand. 2023. Making Sense of Constellations: Methodologies for Understanding Starlink's Scheduling Algorithms. In *Companion of the 19th International Conference on Emerging Networking EXperiments and Technologies* (Paris, France) *(CoNEXT 2023)*. Association for Computing Machinery, New York, NY, USA, 37–43. https://doi.org/10.1145/3624354.3630586

[38] termux. [n. d.]. Android terminal emulator and Linux environment app. https://termux.com/.

[39] The jQuery Foundation. 2025. jQuery: The Write Less, Do More, JavaScript Library. https://jquery.com/ Accessed: 2025-05-15.

[40] Matteo Varvello and Yasir Zaki. 2023. A Worldwide Look Into Mobile Access Networks Through the Eyes of AmiGos. In *2023 7th Network Traffic Measurement and Analysis Conference (TMA)*. 1–10. https://doi.org/10.23919/TMA58422.2023.10198920

[41] Viasat. 2024. *In-Flight Connectivity for Commercial Aviation.* https://www.viasat.com/aviation/commercial-aviation/in-flight-connectivity/

[42] Junyong Wei, Suzhi Cao, Siyan Pan, Jiarong Han, Lei Yan, and Lei Zhang. 2020. SatEdgeSim: A Toolkit for Modeling and Simulation of Performance Evaluation in Satellite Edge Computing Environments. In *2020 12th International Conference on Communication Software and Networks (ICCSN)*. 307–313. https://doi.org/10.1109/ICCSN49894.2020.9139057

[43] Jinwei Zhao and Jianping Pan. 2024. LENS: A LEO Satellite Network Measurement Dataset. In *Proceedings of the 15th ACM Multimedia Systems Conference* (Bari, Italy) *(MMSys '24)*. Association for Computing Machinery, New York, NY, USA, 278–284. https://doi.org/10.1145/3625468.3652170

A ETHICS

The goal of this study is to evaluate in-flight connectivity performance across multiple airlines and technologies, specifically comparing GEO and LEO satellite providers. Study participants were asked to carry our provisioned mobile devices throughout their flights, keep them charged, and, when available, connect them to the onboard Wi-Fi. They were explicitly instructed not to install personal applications, log into any accounts, or store personal data on these devices. Consequently, no personal or sensitive information was recorded at any point during the study.

To ensure ethical compliance, we obtained Institutional Review Board (IRB) approval (anonymized to preserve the double-blind protocol) and two authors completed CITI research-ethics training. All participants reviewed and signed an informed-consent document, with ample opportunity to ask questions about the data being collected.

B APPENDIX

B.1 Starlink Flights

Table 3 provides an overview of the 6 Qatar Airways flights with Starlink connectivity in our dataset. For each flight, we identify the Starlink Points of Presence (PoPs) detected by our measurement endpoints and their respective connection durations in minutes. These durations represent connection periods to our `AmiGo` server only, calculated as the interval between first and last IP reports, excluding any periods when the measurement device was inactive (for example, powered off).

B.2 DNS Configuration for GEO SNOs

Table 4 summarizes the DNS configurations used by different GEO SNOs in our dataset. For each SNO, we identify the DNS hosting provider with the corresponding ASN and the resolver's geolocation. We obseve that some SNOs operate their own DNS infrastructure (e.g., SITA, ViaSat) while others leverage third-party providers like Cloudflare or Google. Temporal changes in DNS configuration are also noted for Panasonic, which switched providers between our measurement periods.

B.3 GEO-based Flights

From December 2023 and March 2025, we conducted network measurements in 20 flights with GEO satellite connectivity. For each of these flights, Table 5 details the origin and destination airports (as IATA codes), departure date, the SNO and its ASN providing connectivity, and PoP location(s).

B.4 Breakdown of TCP file transfer tests

Table 6 summarizes our setup for TCP file transfer tests, where we selected AWS server endpoints based on Starlink PoP in use. Note that Sofia lacks a nearby AWS region, and due to limited connection time in Milan, we were unable to complete Vegas evaluations.

Origin	Destination	Departure Date	PoPs	Duration (minutes)
DOH	JFK	08-03-2025	Doha	74
			Sofia	196
			Warsaw	20
			Frankfurt	46
			London	170
			New York	184
JFK	DOH	16-03-2025	New York	167
			Madrid	55
			Milan	22
			Sofia	172
			Doha	101
DOH	JFK	21-03-2025	Doha	73
			Sofia	189
			Milan	54
			Madrid	45
			London	181
			New York	259
JFK	DOH	07-04-2025	New York	256
			London	143
			Frankfurt	65
			Milan	46
			Sofia	198
			Doha	71
DOHA	LHR	11-04-2025	Doha	79
			Sofia	234
			Warsaw	15
			Frankfurt	64
			London	23
LHR	DOHA	13-04-2025	London	89
			Frankfurt	53
			Milan	22
			Sofia	175
			Doha	88

Table 3: Detail of all Starlink flights in our dataset

SNO	DNS Host	DNS Location
Inmarsat (AS31515)	Cloudflare (AS1335) Packet Clearing House (AS42)	NL, US
Intelsat (AS22351)	Cisco OpenDNS (AS36692)	US
Panasonic (AS64294)	*Cogent Communications (AS174)	US
	**Cloudflare (AS1335) Google (AS15169)	
SITA (AS206433)	SITA (AS206433)	NL
ViaSat (AS40306)	ViaSat (AS7155)	US

* December 2023 - February 2024

** March 2025

Table 4: DNS Providers and resolver locations for GEO SNOs captured in our in-flight dataset

Airline	Origin	Destination	Departure Date	ASN/SNO	PoP Location
AirFrance	BEY	CDG	03-01-2024	AS22351 Intelsat	Wardensville (US)
AirFrance	ATL	CDG	20-01-2024	AS64294 Panasonic	Lake Forest (US)
Emirates	DXB	ADD	22-12-2023	AS206433 SITA	Lelystad (NL)
Emirates	DXB	MEX	23-12-2023	AS206433 SITA	Lelystad (NL)
Emirates	MEX	BCN	01-01-2024	AS206433 SITA	Lelystad (NL)
Emirates	DXB	LHR	03-01-2024	AS206433 SITA	Lelystad (NL)
Emirates	KUL	DXB	02-01-2024	AS206433 SITA	Lelystad (NL)
Etihad	AUH	KUL	21-12-2023	AS64294 Panasonic	Lake Forest (US)
Etihad	ICN	AUH	08-12-2024	AS206433 SITA	Amsterdam (NL)
Etihad	ICN	AUH	07-03-2025	AS64294 Panasonic	Lake Forest (US)
Etihad	FCO	AUH	20-01-2024	AS64294 Panasonic	Lake Forest (US)
Etihad	BKK	AUH	07-01-2024	AS64294 Panasonic	Lake Forest (US)
Etihad	ICN	AUH	03-01-2024	AS64294 Panasonic	Lake Forest (US)
Etihad	AUH	ICN	14-12-2023	AS64294 Panasonic	Lake Forest (US)
Etihad	CDG	AUH	21-01-2024	AS64294 Panasonic	Lake Forest (US)
JetBlue	MIA	KIN	23-12-2023	AS40306 ViaSat	Englewood (US)
KLM	ACC	AMS	02-01-2024	AS22351 Intelsat	Wardensville (US)
Qatar	DOH	MAD	03-11-2024	AS31515 INMARSAT	Staines (GB)
					Greenwich (US)
Qatar	DOH	LAX	08-12-2024	AS206433 SITA	Amsterdam (NL)
SaudiA	DXB	RUH	18-02-2024	AS206433 SITA	Lelystad (NL)

Table 5: Detail of GEO-based flights in our dataset. The origin and destination airports are indicated by IATA codes.

PoP	BBR	Cubic	Vegas
London	London	London	London
Frankfurt	London, Frankfurt	London, Frankfurt	Frankfurt
Milan	Milan	Milan	
Sofia	London		

Table 6: Breakdown of TCP CCA experiments conducted at each PoP, with AWS endpoints colored in orange.